JOURNAL OF SANDWICH STRUCTURES & MATERIALS

Original Article

Journal of Sandwich Structures and Materials
0(0) 1–30

DOI: 10.1177/1099636220979276
journals.sagepub.com/home/jsm
SAGE

Free vibration analysis of rectangular sandwich plates with compressible core and various boundary conditions

Sajjad Riahi Farsani[1], Arash Ramian[1], Ramazan-Ali Jafari-Talookolaei[1], Paolo S Valvo[2] and Maryam Abedi[3]

Abstract

Extended higher-order sandwich plate theory is used to analyze the free vibrations of rectangular sandwich plates with compressible core. Accordingly, first-order shear deformation theory is used to model the laminated face sheets. Besides, the in-plane and transverse displacements of the core are assumed to be cubic and quadratic functions of the thickness coordinate, respectively. To deduce the governing equations, Hamilton's principle is used. Then, based on the Rayleigh-Ritz method, single series expansions with two-variable orthogonal polynomials – namely, the orthogonal plate functions – are considered to approximate the displacement components. Lastly, a generalized eigenvalue problem is solved to obtain the free vibrational characteristics of sandwich plates with both symmetric and anti-symmetric lay-ups subjected to various boundary conditions. The method is validated against the results obtained by different methods in the literature. Finally, the effects of the plate side-to-thickness ratio, in-plane aspect ratio, and core-to-face sheets thickness ratio on the natural frequencies are discussed.

[1]School of Mechanical Engineering, Babol Noshirvani University of Technology, Babol, Iran
[2]Department of Civil and Industrial Engineering, University of Pisa, Pisa, Italy
[3]Department of Mechanical Engineering, Faculty of Engineering and Technology, University of Mazandaran, Babolsar, Iran

Corresponding author:
Ramazan-Ali Jafari-Talookolaei, School of Mechanical Engineering, Babol Noshirvani University of Technology, Shariati Av., 47148-71167 Babol, Mazandaran, Iran.
Email: ramazanali@gmail.com

Keywords
Free vibration, sandwich plate, compressible core, two-variable orthogonal polynomials, orthogonal plate functions, various boundary conditions

Introduction

Today, sandwich plates are used as main structural components in many industrial applications of aerospace, marine, transportation, and civil engineering. A typical sandwich plate is made of two face sheets separated by a core. Face sheets furnish bending strength and stiffness to the sandwich; they are typically made of metals or fiber-reinforced laminates. The core is mainly in charge of bearing the transverse shear. The core material should have low density to reduce the weight of the structure, but sufficiently large transverse Young's modulus to prevent excessive deformation along the thickness. Common technological solutions for the core include honeycomb structures and foam materials [1,2].

Generally speaking, three main approaches have been proposed in the literature to analyze sandwich plates. The first approach uses three-dimensional (3 D) elasticity to evaluate the static and dynamic responses of sandwich plates. Srinivas et al. [3–5] provided exact analytical solutions for the bending, vibration, and buckling problems of homogeneous and laminated thick rectangular plates. Pagano [6] studied the bending behavior of simply supported sandwich plates. Noor et al. [7] used the same method to obtain the free vibration characteristics of sandwich plates.

The second approach includes the so-called equivalent single layer (ESL) theories, whereas the constitutive relations of multi-layered plates are reduced to a single equivalent layer. Accordingly, the core is considered as a layer with different material properties. In the past, attempts have been made to use classical plate theory (CPT) and first-order shear deformation theory (FSDT) to analyze sandwich plates. As expectable, however, classical plate theory does not lead to accurate results since it ignores transverse shear deformation. FSDT predicts constant (averaged) transverse shear stresses in the thickness direction and thus some shear correction factors are needed. To consider variable shear stresses, higher-order shear deformation theories (HSDTs) have been developed. One of the most used HSDTs is the third-order shear deformation theory (TSDT) developed by Reddy [8] for laminated composite plates. Kant and Swaminathan [9,10] used Reddy's TSDT to develop an analytical solution for simply supported sandwich plates. Swaminathan et al. [11,12] adopted the same higher-order theory to study the bending and free vibration problems of sandwich plates with anti-symmetric angle-ply face sheets. Based on Reddy's higher order theory, different finite element analyses have been carried out by, amongst others, Meunier and Shenoi [13]

and Nayak et al. [14]. In the ESL theories, however, deformation of the plate in the thickness direction due to the core compressibility is generally ignored.

The third and last approach includes the layer-wise (LW) theories, whereas each layer (face sheets and core) is considered separately with its own kinematic relations. Rao and Desai [15] provided a higher-order mixed LW model to determine the natural frequencies of simply supported sandwich plates. Bardell et al. [16] obtained the free vibration characteristics of sandwich panels using a zig-zag displacement pattern over the thickness. A modified Fourier–Ritz solution was presented by Yang et al. [17] for the damped vibration analysis of sandwich plates made of viscoelastic and functionally graded materials (FGMs) with various boundary conditions. In their model, FSDT is used for all of the three layers with constant transverse shear deformation. Therefore, only one transverse shear deformation is considered for the face sheets and core, while compatibility conditions between the parts are provided only for the in-plane deformations. Chalak et al. [18] analyzed the free vibrations of soft core sandwich plates using the finite element method (FEM) based on a higher-order zig-zag theory. Frostig and Thomsen [19] developed a higher-order sandwich panel theory (HSAPT), where the layers are interconnected through equilibrium and compatibility conditions. They assumed the core to be compressible, but with negligible in-plane rigidity, and provided two models for this analysis. In the first model, the transverse shear stresses of the core, as well as the displacements of the upper and lower face sheets, are considered as unknowns. In the second model, the displacement field in the core is described by a polynomial based on the displacement field obtained in the first model. In this second model, the polynomial coefficients, along with the displacements of the upper and lower face sheets, are the unknowns. Malekzadeh et al. [20] analyzed the free vibrations of a sandwich plate with simply supported edges using Navier's technique. Malekzadeh and Sayyidmousavi [21] also studied the free vibrations of a sandwich plate with flexible viscoelastic core subjected to various boundary conditions by using a double Fourier series expansion and Stokes's transformation technique. They used FSDT for the face sheets and 3 D elasticity theory for the soft core with out-of-plane stresses only considered. It is worth mentioning that in references [19,21], the shear stresses in the core are assumed constant in the thickness direction. Generally, for the free vibration response, only the out-of-plane stresses are considered, while the in-plane stresses are neglected. Anyway, the HSAPT model is incapable of capturing the in-plane stresses and assumes negligible in-plane rigidity. An extended higher-order sandwich panel theory (EHSAPT) was proposed by Frostig et al. [22] to appropriately take into account the effects of the in-plane and transverse rigidity of the core on the sandwich panel response.

In this paper, we use the well-known Rayleigh-Ritz approximate solution method, originally formulated in 1909 by Ritz [23] and later applied to study the transverse vibration of a square plate with free edges [24]. The method has been used for decades for static, buckling, and free vibration problems of beams, plates, and shells. In the Rayleigh-Ritz method, the displacement parameters representing

the structural response are approximated by (truncated) series expansions with suitable basic functions chosen as terms of the series. For instance, Rahmani et al. [25] used basic functions defined by the product of trigonometric functions for the free vibration analysis of composite sandwich cylindrical shells. Abedi et al. [26] presented a new solution method in which the Legendre orthogonal functions are used as the base function to obtain the vibrational characteristics of laminated composite plates with arbitrary lay-ups and also arbitrary boundary conditions. Bhat [27] studied the vibrations of rectangular plates introducing for the first time the use of double series of one-variable orthogonal polynomials in the plate in-plane coordinates. The first term of such polynomial series for each direction is defined in such a way as to satisfy the essential and natural boundary conditions of the problem. The other polynomials of the series are then obtained by using the Gram-Schmidt process. Bhat [28] also used single series of two-variable orthogonal polynomials to analyze the flexural vibrations of polygonal plates. He also used the Gram-Schmidt process to generate the family of orthogonal polynomials. Liew et al. [29] examined the vibrations of rectangular plates by using a single series of two-variable orthogonal polynomial functions, called orthogonal plate functions, again generated through the Gram-Schmidt process. Liew et al. [30] used the same method for the vibration analysis of skew plates. Later, Nallim et al. [31] presented a general approach for the study of the static and dynamic responses of arbitrary quadrilateral anisotropic plates with various boundary conditions. Nallim and Oller [32] applied this approach for unsymmetrically laminated plates with one-variable orthogonal polynomials to approximate the three components of the displacement field, i.e. the transverse deflection and the two in-plane displacements. Rango et al. [33] investigated the vibrational behavior of quadrilateral laminated composite plates based on TSDT by extending the research of Nallim et al. [31,32]. Kumar and Lal [34] used the Rayleigh-Ritz method with two-variable orthogonal polynomials to study the vibrations of nonhomogeneous orthotropic rectangular plates with bilinear thickness variation resting on a Winkler foundation. Behera and Chakraverty [35] also used this method to analyze the free vibrations of rectangular nano-plates. Recently, Kumar [36] provided a comprehensive review of the literature on the Rayleigh-Ritz method and its application to various beam, plate, and shell problems. Moreno-García et al. [37] also reviewed the literature and used the Rayleigh-Ritz method to solve plate and beam problems. Orthogonal polynomials, non-orthogonal polynomials, and trigonometric functions have been proposed as basic functions of the series expansion. In particular, orthogonal polynomial functions have proven to enable rapid convergence of the method. Nallim and Grossi [38] demonstrated that the Rayleigh-Ritz method with orthogonal polynomials functions is very satisfactory for anisotropic plates, whereas faster convergence is achieved with respect to non-orthogonal polynomial. Besides orthogonality, the use of single series instead of double series also reduces computational costs. Another advantage of using polynomial functions is that they can be easily defined in such a way as to satisfy the essential boundary conditions.

Based on the above, we use single series with two-variable orthogonal polynomials (orthogonal plate functions) to apply the Rayleigh-Ritz method. As an improvement with respect to previous researches, we consider the core to be compressible and subjected to all of the in-plane and out-of-plane stress components. The face sheets are assumed to be made of fiber-reinforced composite laminates. Accordingly, FSDT is used for the face sheets and the second model by Frostig and Thomsen [19] is used for the core. Furthermore, the solution method is presented in such a way that it is possible to obtain results for arbitrary boundary conditions.

The paper is organized as follows. In the next section, the mathematical formulation of the problem is given starting from plate kinematics and arriving at the expressions for the kinetic and strain energies. Then, the solution method is presented: based on the Rayleigh-Ritz method, a generalized eigenvalue problem is formulated, whose solution yields the natural frequencies and mode shapes of the plate. Next, numerical results are given and discussed: first, a convergence study is performed and the proposed method is validated through comparison with other methods of the literature; then, some example problems are analyzed for sandwich plates with both symmetric and anti-symmetric lay-ups. The effects on the natural frequencies of the plate in-plane aspect ratio, boundary conditions, plate side-to-thickness ratio, and core-to-face sheets thickness ratio are investigated.

Mathematical formulation

Kinematics

Let us consider a rectangular sandwich plate of length a, width b, and total thickness h (Figure 1). The plate is made up of three layers, namely a top face sheet with thickness f_t, a core with thickness f_c, and a bottom face sheet with thickness f_b. In the following, the indices t, c, and b will refer to the top face, core, and bottom face, respectively. Let us introduce a global Cartesian reference system $Oxyz$ with the origin at a vertex of the top face sheet, the x- and y-axes aligned with the plate length and width directions, respectively, and the z-axis pointing downwards.

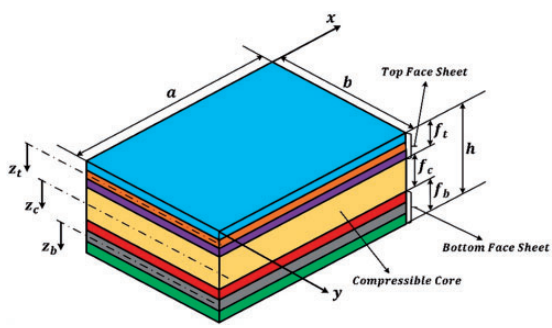

Figure 1. Sandwich plate with length a, width b, and total thickness h.

Parallel to the global z-axis, we introduce local z_α-axes ($\alpha = t,\ c,\ b$) with their origins at the mid-planes of the top face sheet, core, and bottom face sheet, respectively.

Based on FSDT and assuming harmonic free vibrations with angular frequency $\bar{\omega}$, the displacement components at an arbitrary point with coordinates (x, y, z) of the top and bottom face sheets at time t can be written as follows:

$$\begin{cases} u_\alpha(x,y,z,t) = [u_0^\alpha(x,y) + z_\alpha \psi_x^\alpha(x,y)]\exp(\hat{j}\bar{\omega}t) \\ v_\alpha(x,y,z,t) = [v_0^\alpha(x,y) + z_\alpha \psi_y^\alpha\Big(x,y)]\exp(\hat{j}\bar{\omega}t)\,, \quad (\alpha = t,b) \\ w_\alpha(x,y,t) = w_0^\alpha(x,y)\exp(\hat{j}\bar{\omega}t) \end{cases} \tag{1}$$

where u_0^α and v_0^α are the in-plane displacements (in the x- and y-directions, respectively), w_0^α is the transverse displacement (in the z-direction) of the middle surface of the face sheets, ψ_x^α and ψ_y^α are the rotation angles of the transverse normal about the y- and x-directions, respectively. Furthermore, $\hat{j}$ denotes the imaginary unit.

In what follows, we drop the dependence on time and focus on the mode shapes. By assuming small deformations, the strain-displacement relations for the face sheets are as follows:

$$\begin{aligned} &\varepsilon_{xx}^\alpha(x,y,z_i) = u_{0,x}^\alpha + z_\alpha \psi_{x,x}^\alpha = \varepsilon_{0xx}^\alpha + z_\alpha \kappa_x^\alpha \\ &\varepsilon_{yy}^\alpha(x,y,z_i) = v_{0,y}^\alpha + z_\alpha \psi_{y,y}^\alpha = \varepsilon_{0yy}^\alpha + z_\alpha \kappa_y^\alpha \\ &\gamma_{xy}^\alpha(x,y,z_i) = u_{0,y}^\alpha + v_{0,x}^\alpha + z_\alpha\big(\psi_{x,y}^\alpha + \psi_{y,x}^\alpha\big) = \gamma_{0xy}^\alpha + z_\alpha \kappa_{xy}^\alpha \\ &\gamma_{xz}^\alpha(x,y,z_i) = \psi_x^\alpha + w_{0,x}^\alpha \\ &\gamma_{yz}^\alpha(x,y,z_i) = \psi_y^\alpha + w_{0,y}^\alpha \ \ (\alpha = t,b) \end{aligned} \tag{2}$$

where a comma in the subscript denotes differentiation with respect to the following variable, also the following strain measures have been defined:

$$\begin{aligned} &\varepsilon_{0xx}^\alpha = u_{0,x}^\alpha \\ &\varepsilon_{0yy}^\alpha = v_{0,y}^\alpha \\ &\gamma_{0xy}^\alpha = u_{0,y}^\alpha + v_{0,x}^\alpha \\ &\kappa_x^\alpha = \psi_{x,x}^\alpha \\ &\kappa_y^\alpha = \psi_{y,y}^\alpha \\ &\kappa_{xy}^\alpha = \psi_{x,y}^\alpha + \psi_{y,x}^\alpha \ \ (\alpha = t,b) \end{aligned} \tag{3}$$

For the displacement field of the core, the second model provided by Frostig and Thomsen [19] is used. To consider the effects of core compression, the in-plane displacements are assumed to be cubic functions of the transverse coordinate, while the transverse displacement is assumed to vary quadratically in the thickness

direction. Based on EHSAPT, the displacement components for the core can be written as follows:

$$\begin{aligned} u_c(x,y,z_c) &= u_0(x,y) + z_c u_1(x,y) + z_c^2 u_2(x,y) + z_c^3 u_3(x,y) \\ v_c(x,y,z_c) &= v_0(x,y) + z_c v_1(x,y) + z_c^2 v_2(x,y) + z_c^3 v_3(x,y) \\ w_c(x,y,z_c) &= w_0(x,y) + z_c w_1(x,y) + z_c^2 w_2(x,y) \end{aligned} \tag{4}$$

In the above equation, u_0 and v_0 are the in-plane displacements (in the x- and y-directions, respectively) and w_0 is the tranverse displacement (in the z-direction) of the core middle surface. Besides, u_1 and v_1 are the rotation angles of the transverse normal about the y- and x-axes, respectively. The functions u_2, u_3, v_2, v_3, w_1 and w_2 are generalized displacements, which will be calculated using the compatibility conditions between the core and the face sheets.

The strain-displacement relations for the core can be written out as follows:

$$\begin{aligned} \varepsilon^c_{xx} &= u_{0,x} + z_c u_{1,x} + {z_c}^2 u_{2,x} + {z_c}^3 u_{3,x} \\ \varepsilon^c_{yy} &= v_{0,y} + z_c v_{1,y} + {z_c}^2 v_{2,y} + {z_c}^3 v_{3,y} \\ \varepsilon^c_{zz} &= w_1 + 2z_c w_2 \\ \gamma^c_{xy} &= u_{0,y} + z_c u_{1,y} + {z_c}^2 u_{2,y} + {z_c}^3 u_{3,y} + v_{0,x} + z_c v_{1,x} + {z_c}^2 v_{2,x} + {z_c}^3 v_{3,x} \\ \gamma^c_{xz} &= u_1 + 2z_c u_2 + 3{z_c}^2 u_3 + w_{0,x} + z_c w_{1,x} + {z_c}^2 w_{2,x} \\ \gamma^c_{yz} &= v_1 + 2z_c v_2 + 3{z_c}^2 v_3 + w_{0,y} + z_c w_{1,y} + {z_c}^2 w_{2,y} \end{aligned} \tag{5}$$

Similar to equation (3), the following generalized strain measures can be defined:

$$\begin{aligned} &\varepsilon^c_{0xx} = u_{0,x}; \quad \varepsilon^c_{1xx} = u_{1,x}; \quad \varepsilon^c_{2xx} = u_{2,x}; \quad \varepsilon^c_{3xx} = u_{3,x} \\ &\varepsilon^c_{0yy} = v_{0,x}; \quad \varepsilon^c_{1yy} = v_{1,x}; \quad \varepsilon^c_{2yy} = v_{2,x}; \quad \varepsilon^c_{3yy} = v_{3,x} \\ &\varepsilon^c_{0zz} = w_1; \quad \varepsilon^c_{1zz} = 2w_2; \quad \gamma^c_{0xy} = u_{0,y} + v_{0,x}; \quad \gamma^c_{1xy} = u_{1,y} + v_{1,x} \\ &\gamma^c_{2xy} = u_{2,y} + v_{2,x}; \quad \gamma^c_{3xy} = u_{3,y} + v_{3,x}; \quad \gamma^c_{0xz} = u_1 + w_{0,x} \\ &\gamma^c_{1xz} = 2u_2 + w_{1,x}; \quad \gamma^c_{2xz} = 3u_3 + w_{2,x}; \quad \gamma^c_{0yz} = v_1 + w_{0,y} \\ &\gamma^c_{1yz} = 2v_2 + w_{1,y}; \quad \gamma^c_{2yz} = 3v_3 + w_{2,y} \end{aligned} \tag{6}$$

Constitutive equations and stress resultants

The strain-stress relations for the k-th layer of the top or bottom laminated face sheets are given by [39]:

$$\begin{Bmatrix} \sigma_{xx} \\ \sigma_{yy} \\ \tau_{xy} \end{Bmatrix}_k = \begin{bmatrix} \bar{Q}_{11} & \bar{Q}_{12} & \bar{Q}_{16} \\ \bar{Q}_{12} & \bar{Q}_{22} & \bar{Q}_{26} \\ \bar{Q}_{16} & \bar{Q}_{26} & \bar{Q}_{66} \end{bmatrix}_k \begin{Bmatrix} \varepsilon_{xx} \\ \varepsilon_{yy} \\ \gamma_{xy} \end{Bmatrix}_k, \quad \begin{Bmatrix} \tau_{yz} \\ \tau_{xz} \end{Bmatrix}_k = \begin{bmatrix} \bar{Q}_{44} & \bar{Q}_{45} \\ \bar{Q}_{45} & \bar{Q}_{55} \end{bmatrix}_k \begin{Bmatrix} \gamma_{yz} \\ \gamma_{xz} \end{Bmatrix}_k \tag{7}$$

where $(\bar{Q}_{ij})_k$ are the transformed stiffness constants of the k-th layer. The stress resultants for the face sheets are related to the generalized displacements as follows:

$$\begin{Bmatrix} N^{\alpha}_{xx} \\ N^{\alpha}_{yy} \\ N^{\alpha}_{xy} \end{Bmatrix} = \begin{bmatrix} A^{\alpha}_{11} & A^{\alpha}_{12} & A^{\alpha}_{16} \\ A^{\alpha}_{21} & A^{\alpha}_{22} & A^{\alpha}_{26} \\ A^{\alpha}_{16} & A^{\alpha}_{26} & A^{\alpha}_{66} \end{bmatrix} \begin{Bmatrix} u^{\alpha}_{0,x} \\ v_{0,y} \\ u^{\alpha}_{0,y} + v^{\alpha}_{0,x} \end{Bmatrix} + \begin{bmatrix} B^{\alpha}_{11} & B^{\alpha}_{12} & B^{\alpha}_{16} \\ B^{\alpha}_{21} & B^{\alpha}_{22} & B^{\alpha}_{26} \\ B^{\alpha}_{16} & B^{\alpha}_{26} & B^{\alpha}_{66} \end{bmatrix} \begin{Bmatrix} \psi^{\alpha}_{x,x} \\ \psi^{\alpha}_{y,y} \\ \psi^{\alpha}_{x,y} + \psi^{\alpha}_{y,x} \end{Bmatrix} \quad (\alpha = t, b) \tag{8}$$

$$\begin{Bmatrix} M^{\alpha}_{xx} \\ M^{\alpha}_{yy} \\ M^{\alpha}_{xy} \end{Bmatrix} = \begin{bmatrix} B^{\alpha}_{11} & B^{\alpha}_{12} & B^{\alpha}_{16} \\ B^{\alpha}_{21} & B^{\alpha}_{22} & B^{\alpha}_{26} \\ B^{\alpha}_{16} & B^{\alpha}_{26} & B^{\alpha}_{66} \end{bmatrix} \begin{Bmatrix} u^{\alpha}_{0,x} \\ v^{\alpha}_{0,y} \\ u^{\alpha}_{0,y} + v^{\alpha}_{0,x} \end{Bmatrix} + \begin{bmatrix} D^{\alpha}_{11} & D^{\alpha}_{12} & D^{\alpha}_{16} \\ D^{\alpha}_{21} & D^{\alpha}_{22} & D^{\alpha}_{26} \\ D^{\alpha}_{16} & D^{\alpha}_{26} & D^{\alpha}_{66} \end{bmatrix} \begin{Bmatrix} \psi^{\alpha}_{x,x} \\ \psi^{\alpha}_{y,y} \\ \psi^{\alpha}_{x,y} + \psi^{\alpha}_{y,x} \end{Bmatrix} \quad (\alpha = t, b) \tag{9}$$

$$\begin{Bmatrix} Q^{\alpha}_{yz} \\ Q^{\alpha}_{xz} \end{Bmatrix} = \begin{bmatrix} A^{\alpha}_{44} & A^{\alpha}_{45} \\ A^{\alpha}_{45} & A^{\alpha}_{55} \end{bmatrix} \begin{Bmatrix} w_{\alpha,y} + \psi^{\alpha}_{y} \\ w_{\alpha,x} + \psi^{\alpha}_{x} \end{Bmatrix} \quad (\alpha = t, b) \tag{10}$$

where A^{α}_{ij}, B^{α}_{ij}, and D^{α}_{ij} $(i,j = 1,2,6)$ are the components of the extensional, extensional-bending coupling, and bending stiffness matrices, respectively. Likewise, A^{α}_{ij} $(i,j = 4,5)$ are the components of the transverse shear stiffness matrices. Such components are given by:

$$A^{\alpha}_{ij} = \sum_{k=1}^{N} \left(\bar{Q}_{ij}\right)_k (z_{\alpha k} - z_{\alpha(k-1)}) \tag{11a}$$

$$B^{\alpha}_{ij} = \frac{1}{2} \sum_{k=1}^{N} \left(\bar{Q}_{ij}\right)_k (z^2_{\alpha k} - z^2_{\alpha(k-1)}) \tag{11b}$$

$$D^{\alpha}_{ij} = \frac{1}{3} \sum_{k=1}^{N} \left(\bar{Q}_{ij}\right)_k (z^3_{\alpha k} - z^3_{\alpha(k-1)}) \tag{11c}$$

in which N is the total number of layers in the laminate, $z_{\alpha k}$ and $z_{\alpha(k-1)}$ are the distances of the top and bottom surfaces of the k-th layer from the face sheet mid-plane, respectively.

Besides, by assuming that the core material is orthotropic, the stress-strain relations for it can be written as follows:

$$\begin{Bmatrix} \sigma_{xx}^c \\ \sigma_{yy}^c \\ \sigma_{zz}^c \\ \tau_{xz}^c \\ \tau_{yz}^c \\ \tau_{xy}^c \end{Bmatrix} = \begin{bmatrix} \frac{1}{E_1} & -\frac{\upsilon_{12}}{E_1} & -\frac{\upsilon_{13}}{E_1} & 0 & 0 & 0 \\ -\frac{\upsilon_{12}}{E_1} & \frac{1}{E_2} & -\frac{\upsilon_{23}}{E_2} & 0 & 0 & 0 \\ -\frac{\upsilon_{13}}{E_1} & -\frac{\upsilon_{23}}{E_2} & \frac{1}{E_3} & 0 & 0 & 0 \\ 0 & 0 & 0 & \frac{1}{G_{23}} & 0 & 0 \\ 0 & 0 & 0 & 0 & \frac{1}{G_{31}} & 0 \\ 0 & 0 & 0 & 0 & 0 & \frac{1}{G_{12}} \end{bmatrix}^{-1} \begin{Bmatrix} \varepsilon_{xx}^c \\ \varepsilon_{yy}^c \\ \varepsilon_{zz}^c \\ \gamma_{xz}^c \\ \gamma_{yz}^c \\ \gamma_{xy}^c \end{Bmatrix} \tag{12}$$

where E_i, υ_{ij}, and G_{ij} are the Young's moduli, Poisson's ratios, and shear moduli in the material principal reference system, and the superscript –1 denotes matrix inversion.

The stress resultants of the core are given by:

$$\begin{aligned} \{N_{xx}^c, M_{mxx}^c\} &= \int_{-\frac{f_c}{2}}^{\frac{f_c}{2}} (1, z_c^m)\sigma_{xx}^c \mathrm{d}z_c \\ \{N_{yy}^c, M_{myy}^c\} &= \int_{-\frac{f_c}{2}}^{\frac{f_c}{2}} (1, z_c^m)\sigma_{yy}^c \mathrm{d}z_c \\ \{N_{xy}^c, M_{mxy}^c\} &= \int_{-\frac{f_c}{2}}^{\frac{f_c}{2}} (1, z_c^m)\tau_{xy}^c \mathrm{d}z_c \ \ (m = 1,2,3) \\ \{Q_{xz}^c, M_{Qnxz}^c\} &= \int_{-\frac{f_c}{2}}^{\frac{f_c}{2}} (1, z_c^n)\tau_{xz}^c \mathrm{d}z_c \ \ (n = 1,2) \\ \{Q_{yz}^c, M_{Qnyz}^c\} &= \int_{-\frac{f_c}{2}}^{\frac{f_c}{2}} (1, z_c^n)\tau_{yz}^c \mathrm{d}z_c \\ \{R_z^c, M_z^c\} &= \int_{-\frac{f_c}{2}}^{\frac{f_c}{2}} (1, z_c)\sigma_{zz}^c \mathrm{d}z_c \end{aligned} \tag{13}$$

Strain and kinetic energies

The maximum strain energy of the top and bottom face sheets can be calculated as follows:

$$\begin{aligned} U_\alpha = \frac{1}{2}\int_0^a \int_0^b [&N_{xx}^\alpha \varepsilon_{0xx}^\alpha + N_{yy}^\alpha \varepsilon_{0yy}^\alpha + N_{xy}^\alpha \gamma_{0xy}^\alpha + M_{xx}^\alpha \kappa_x^\alpha + M_{yy}^\alpha \kappa_y^\alpha \\ &+ M_{xy}^\alpha \kappa_{xy}^\alpha + Q_{yz}^\alpha \gamma_{yz}^\alpha + Q_{xz}^\alpha \gamma_{xz}^\alpha] \mathrm{d}y\mathrm{d}x \ \ (\alpha = t, b) \end{aligned} \tag{14}$$

where the stress resultants and strain measures are given by equations (8) to (10) and (3), respectively.

Likewise, the maximum strain energy of the core can be calculated as:

$$U_c = \frac{1}{2}\int_0^a \int_0^b (N^c_{xx}\varepsilon^c_{0xx} + M^c_{1xx}\varepsilon^c_{1xx} + M^c_{2xx}\varepsilon^c_{2xx} + M^c_{3xx}\varepsilon^c_{3xx} + N^c_{yy}\varepsilon^c_{0yy} + M^c_{1yy}\varepsilon^c_{1yy} + M^c_{2yy}\varepsilon^c_{2yy} + M^c_{3yy}\varepsilon^c_{3yy} + R^c_z\varepsilon^c_{0zz} + M^c_z\varepsilon^c_{1zz} + N^c_{xy}\gamma^c_{0xy} + M^c_{1xy}\gamma^c_{1xy} + M^c_{2xy}\gamma^c_{2xy} + M^c_{3xy}\gamma^c_{3xy} + Q^c_{xz}\gamma^c_{0xz} + M^c_{Q1xz}\gamma^c_{1xz} + M^c_{Q2xz}\gamma^c_{2xz} + Q^c_{yz}\gamma^c_{0yz} + M^c_{Q1yz}\gamma^c_{1yz} + M^c_{Q2yz}\gamma^c_{2yz})\mathrm{d}y\mathrm{d}x \tag{15}$$

where the stress resultants and strain measures are given by equations (14) and (6), respectively.

Also, the maximum kinetic energy of the top and bottom face sheets and core can be computed as follows:

$$T_\alpha = \frac{1}{2}\int_0^a \int_0^b \left[I^\alpha_0\left((u^\alpha_0)^2 + (v^\alpha_0)^2 + (w^\alpha_0)^2\right) + 2I^\alpha_1\left(u^\alpha_0\psi^\alpha_x + v^\alpha_0\psi^\alpha_y\right) + I^\alpha_2\left(\left(\psi^\alpha_x\right)^2 + \left(\psi^\alpha_y\right)^2\right)\right]\mathrm{d}y\mathrm{d}x \quad (\alpha = t, b) \tag{16}$$

and

$$T_c = \frac{1}{2}\int_0^a \int_0^b \Big[I^c_0\left({w_0}^2 + {u_0}^2 + {v_0}^2\right) + 2I^c_1(w_0w_1 + v_0v_1 + u_0u_1) + I^c_2\left({w_1}^2 + 2w_0w_2 + {v_1}^2 + 2v_0v_2 + {u_1}^2 + 2u_0u_2\right) + 2I^c_3(w_1w_2 + v_1v_2 + v_0v_3 + u_1u_2 + u_0u_3) + I^c_4\left({w_2}^2 + {v_2}^2 + 2v_1v_3 + {u_2}^2 + 2u_1u_3\right) + 2I^c_5(v_2v_3 + u_2u_3) + I^c_6({u_3}^2 + {v_3}^2)\Big]\mathrm{d}y\ \mathrm{d}x \tag{17}$$

where

$$\begin{aligned}(I^\alpha_0, I^\alpha_1, I^\alpha_2) &= \textstyle\int_{-f_\alpha/2}^{f_\alpha/2} \rho^\alpha(1, z_\alpha, z^2_\alpha)dz_\alpha \ \ (i = t, b)\\ (I^c_0, I^c_1, I^c_2, I^c_3, I^c_4, I^c_5, I^c_6) &= \textstyle\int_{-f_c/2}^{f_c/2} \rho^c(1, z_c, z^2_c, z^3_c, z^4_c, z^5_c, z^6_c)dz_c\end{aligned} \tag{18}$$

are the inertia terms of the face sheets and core.

The total strain energy and kinetic energy of the sandwich plate are equal to the sum of the strain and kinetic energies, respectively, of the face sheets and core:

$$U_{Total} = U_c + U_t + U_b \tag{19}$$

and

$$T_{Total} = T_c + T_t + T_b \tag{20}$$

The governing equations and boundary conditions can be derived through Hamilton's principle, as presented in Appendix 2.

Compatibility conditions

Assuming complete bond with no slip between the core and face sheets, the compatibility conditions at the upper and lower face–core interfaces read as follows:

$$u_c\left(z_c = -\frac{f_c}{2}\right) = u_0^t + \frac{1}{2}f_t\psi_x^t \quad v_c\left(z_c = -\frac{f_c}{2}\right) = v_0^t + \frac{1}{2}f_t\psi_y^t \quad w_c\left(z_c = -\frac{f_c}{2}\right) = w_0^t \tag{21}$$

and

$$u_c\left(z_c = \frac{f_c}{2}\right) = u_0^b - \frac{1}{2}f_b\psi_x^b \;\; v_c\left(z_c = \frac{f_c}{2}\right) = v_0^b - \frac{1}{2}f_b\psi_y^b \;\; w_c\left(z_c = \frac{f_c}{2}\right) = w_0^b \tag{22}$$

By substituting equations (1) and (4) into the above equations, the compatibility conditions are obtained:

$$\begin{aligned}
&u_0 + u_1\frac{f_c}{2} + u_2\frac{f_c^2}{4} + u_3\frac{f_c^3}{8} = u_0^b - \psi_x^b\frac{f_b}{2}\\
&v_0 + v_1\frac{f_c}{2} + v_2\frac{f_c^2}{4} + v_3\frac{f_c^3}{8} = v_0^b - \psi_y^b\frac{f_b}{2}\\
&w_0 + w_1\frac{f_c}{2} + w_2\frac{f_c^2}{4} = w_0^b\\
&u_0 - u_1\frac{f_c}{2} + u_2\frac{f_c^2}{4} - u_3\frac{f_c^3}{8} = u_0^t + \psi_x^t\frac{f_t}{2}\\
&v_0 - v_1\frac{f_c}{2} + v_2\frac{f_c^2}{4} - v_3\frac{f_c^3}{8} = v_0^t + \psi_y^t\frac{f_t}{2}\\
&w_0 - w_1\frac{f_c}{2} + w_2\frac{f_c^2}{4} = w_0^t
\end{aligned} \tag{23}$$

For the ease of calculation, the relations between the dependent coefficients are calculated, so that the number of unknowns of the problem is reduced.

The relations between the displacement-dependent parameters in the core are derived as follows:

$$\begin{aligned}
u_2 &= (2(u_0^b + u_0^t) - f_b\psi_x^b + f_t\psi_x^t - 4u_0)/f_c^2 \\
u_3 &= (4(u_0^b - u_0^t) - 2\left(f_b\psi_x^b + f_t\psi_x^{\mathrm{t}}\right) - 4f_c u_1)/f_c^3 \\
v_2 &= (2(v_0^b + v_0^t) - f_b\psi_y^b + f_t\psi_y^t - 4v_0)/f_c^2 \\
v_3 &= (4(v_0^b - v_0^t) - 2\left(f_b\psi_y^b + f_t\psi_y^t\right) - 4f_c v_1)/f_c^3 \\
w_2 &= 2(w_0^b + w_0^t - 2w_0)/f_c^2 \\
w_1 &= (w_0^b - w_0^t)/f_c
\end{aligned} \tag{24}$$

Solution method

Series expansion of generalized displacements

The displacement components are approximated by using m-term truncated single series of two-variable orthogonal polynomials:

$$\begin{aligned}
w_0^t(x,y) &= \sum_{i=1}^{m} A_i\phi_i^{w^t}(x,y) \quad v_0^t(x,y) = \sum_{i=1}^{m} B_i\phi_i^{v^t}(x,y) \\
u_0^t(x,y) &= \sum_{i=1}^{m} C_i\phi_i^{u^t}(x,y) \quad \psi_x^t(x,y) = \sum_{i=1}^{m} D_i\phi_i^{x^t}(x,y) \\
\psi_y^t(x,y) &= \sum_{i=1}^{m} E_i\phi_i^{y^t}(x,y) \quad w_0^b(x,y) = \sum_{i=1}^{m} F_i\phi_i^{w^b}(x,y) \\
v_0^b(x,y) &= \sum_{i=1}^{m} G_i\phi_i^{v^b}(x,y) \quad u_0^b(x,y) = \sum_{i=1}^{m} H_i\phi_i^{u^b}(x,y) \\
\psi_x^b(x,y) &= \sum_{i=1}^{m} I_i\phi_i^{x^b}(x,y) \quad \psi_y^b(x,y) = \sum_{i=1}^{m} J_i\phi_i^{y^b}(x,y) \\
w_0(x,y) &= \sum_{i=1}^{m} K_i\phi_i^{w^c}(x,y) \quad v_0(x,y) = \sum_{i=1}^{m} L_i\phi_i^{v^c}(x,y) \\
u_0(x,y) &= \sum_{i=1}^{m} M_i\phi_i^{u^c}(x,y) \quad v_1(x,y) = \sum_{i=1}^{m} N_i\phi_i^{v_1{}^c}(x,y) \\
u_1(x,y) &= \sum_{i=1}^{m} O_i\phi_i^{u_1{}^c}(x,y)
\end{aligned} \tag{25}$$

where $A_i, B_i, C_i, D_i, E_i, F_i, G_i, H_i, I_i, J_i, K_i, L_i, M_i, O_i$ $(i = 1,2,\ldots,m)$ are unknown coefficients and $\phi_i^k (k = w^t, w^b, w^c, \ldots, u_1{}^c)$ are the shape functions. The latter have to be chosen in such a way as to satisfy the essential boundary conditions. To this aim, the first member of the orthogonal polynomial basis ϕ_1^k is defined as

described in Appendix 1. The other members of the orthogonal polynomial basis are generated through the following recursive formula [25,26]:

$$\phi_i^k(x,y) = \big(f_i(x,y) - a_{i,1}\big)\phi_1^k(x,y) - a_{i,2}\phi_2^k(x,y) - a_{i,3}\phi_3^k(x,y) - \cdots - a_{i,i-1}\phi_{i-1}^k(x,y) \tag{26}$$

where $f_i(x,y)$ are weight functions (represented by $1, x, y, x^2, xy, y^2, \ldots, x^{i-n}y^n$ with $i = 1, \ldots, m$ and $n = 0, \ldots, m$) and $a_{i,i-1}$ are calculated as follows [28,29]:

$$a_{i.i-1} = \frac{\int_0^a \int_0^b f_i \phi_1^k(x,y)\phi_{i-1}^k(x,y)\ \mathrm{d}y\mathrm{d}x}{\int_0^a \int_0^b \phi_{i-1}^k(x,y)\phi_{i-1}^k(x,y)\ \mathrm{d}y\mathrm{d}x} \tag{27}$$

Using the above relations, the basic functions are created with the following orthogonality properties:

$$\int_0^a \int_0^b \phi_i^k(x,y)\phi_j^k(x,y)\mathrm{d}x\mathrm{d}y = \begin{cases} 0 \text{ if } i \neq j \\ \\ \epsilon_{ij} \neq 0 \text{ if } i = j \end{cases} \tag{28}$$

Generalized eigenvalue problem

Based on the Rayleigh-Ritz method, the difference between the maximum strain and kinetic energies (19) and (20) is minimized with respect to the unknown coefficients:

$$\frac{\partial(U_{Total} - T_{Total})}{\partial(A_i, B_i, C_i, D_i, E_i, F_i, G_i, H_i, I_i, J_i, K_i, L_i, M_i, O_i)} = 0 \tag{29}$$

The matrix form of the abovementioned equations is:

$$\big([K] - \bar{\omega}^2[M]\big)\begin{Bmatrix} A_i \\ B_i \\ C_i \\ D_i \\ E_i \\ F_i \\ G_i \\ H_i \\ I_i \\ J_i \\ K_i \\ L_i \\ M_i \\ N_i \\ O_i \end{Bmatrix} = \{0\} \tag{30}$$

Table 1. Material properties adopted for the example sandwich plates.

		Material no.					
Property	Unit	M_1 [20]	M_2 [20]	M_3 [18]	M_4 [18]	M_5 [18]	M_6 [18]
E_1	GPa	0.10363	24.51	0.5776	276	0.00689	131
E_2	GPa	0.10363	7.77	0.5776	6.9	0.00689	10.34
E_3	GPa	0.10363	7.77	0.5776	6.9	0.00689	10.34
G_{12}	GPa	0.05	3.34	0.1079	6.9	0.00345	6.895
G_{23}	GPa	0.05	1.34	0.2221	6.9	0.00345	6.895
G_{13}	GPa	0.05	3.34	0.1079	6.9	0.00345	6.205
v_{12}		0.33	0.078	0.0025	0.25	0	0.22
v_{23}		0.33	0.49	0.0025	0.25	0	0.22
v_{13}		0.33	0.078	0.0025	0.3	0	0.49
ρ	kg/m^3	130	1800	1000	681.8	97	1627

Equation (30) represents a generalized eigenvalue problem, out of which one can obtain the natural frequencies (eigenvalues) and mode shapes (eigenvectors) of the sandwich plate.

Results and discussion

Material properties and plate lay-ups

Table 1 shows the material properties adopted for the core and face sheets of the sandwich plates analyzed in the following examples.

The following four lay-ups will be considered in the examples (the angles in degrees represent fiber orientations with respect to the x-axis, C represents the core):

- lay-up #1) 0°/90°/0°/C/0°/90°/0°: a seven–layer symmetric sandwich plate with core thickness 0.88h, material 1 for the core and material 2 for the laminated face sheets;
- lay-up #2) 45°/–45°/45°/C/–45°/45°/–45°: a seven-layer anti-symmetric sandwich plate with core thickness 0.88h, material 1 for the core and material 2 for the laminated face sheets;
- lay-up #3) 0°/90°/C/90°/0°: a five-layer symmetric sandwich plate with core thickness 0.8h, material 3 for the core and material 4 for the laminated face sheets;
- lay-up #4) 0°/90°/C/0°/90°: a five-layer anti-symmetric sandwich plate with core thickness 0.8h, material 5 for the core and material 6 for the laminated face sheets.

Convergence study

In the proposed method, the number of terms of the truncated series plays a crucial role for the accuracy of numerical results. Table 2 shows the first six dimensionless

Table 2. Convergence study of first six dimensionless natural frequencies. $\omega = \bar{\omega}a^2\sqrt{\rho_c/E_c}/h$ of a simply supported sandwich plate with $a/b = 1, a/h = 10$ and. $h_c/h = 0.88$.

	Dimensionless natural frequencies					
M	ω_1	ω_2	ω_3	ω_4	ω_5	ω_6
10	14.2844	27.6400	28.1594	36.4457	42.7456	42.8172
15	14.2843	26.2126	26.8479	36.2009	42.0549	42.8656
20	14.2827	26.2122	26.8455	34.5758	40.7453	41.9713
25	14.2820	26.2086	26.8224	34.5695	39.2526	40.0359
30	14.2820	26.1842	26.8222	34.5591	39.2287	39.9286
35	14.2820	26.1842	26.8222	34.5165	39.2213	39.9226
40	14.2820	26.1842	26.8221	34.5165	39.1128	39.9223
45	14.2820	26.1842	26.8221	34.5165	39.1128	39.9223

Table 3. Dimensionless natural frequencies for seven-layer simply supported sandwich plates with different lay-ups, $a/b = 1$, $a/h = 10$, and $h_c/h = 0.88$.

		Method					
Lay-ups	Mode No.	Present (with in-plane)	Present (without in-plane)	Analytical [20]	FEM-HSDT (LW) [40]	Analytical-HSDT (ESL) [13]	FEM–HSDT (ESL) [14]
#1	ω_1	14.282	14.3404	14.83	14.440	15.28	15.34
	ω_2	26.1842	26.5028	26.91	26.826	28.69	30.18
	ω_3	26.8221	27.1551	27.47	27.456	30.01	31.96
	ω_4	34.5165	35.2757	35.57	35.706	38.86	40.94
#2	ω_1	15.245	15.312	15.53	15.405	16.38	16.43
	ω_2	26.7295	27.0592	27.36	27.417	29.65	31.17
	ω_3	26.7295	27.0592	27.36	27.417	29.65	31.17
	ω_4	35.3905	36.1435	36.93	36.592	40	42.78

natural frequencies, $\omega = \bar{\omega}a^2\sqrt{\rho_c/E_c}/h$, calculated for a simply supported sandwich plate with a different number of series terms. Here, ρ_c and E_c are the density and Young's modulus of the core, respectively; $\bar{\omega}$ and h respectively are the natural frequency and total thickness of the plate. After considering a number of terms equal to forty, the response of the first four natural frequencies converged to the fourth decimal digit. Therefore, in all of the subsequent analyses the number of terms is chosen to be $m = 40$.

Validation

As discussed in the literature review, in previous researches, the natural frequencies of simply supported sandwich plates have been obtained using several analytical and numerical methods. In Table 3, a comparison of results is presented for

Table 4. Dimensionless natural frequencies for symmetric five-layer sandwich plates with lay-up #3, different boundary conditions, $a/b = 1$, $a/h = 10$, and $h_c/h = 0.8$.

		Frequencies					
B.C.	Method	ω_1	ω_2	ω_3	ω_4	ω_5	ω_6
CFCF	Present	7.0426	7.7690	14.2215	15.2980	17.1898	21.5046
	Chalak [18]	7.0359	7.7249	14.2105	15.2415	17.1179	21.3580
	3D Abaqus [41]	7.0119	7.7131	14.1496	15.1975	17.0942	21.3089
	ZIGT FE [41]	7.0923	7.8284	14.3407	15.4498	17.1776	21.5871
CFFF	Present	2.9740	3.6312	9.4107	10.7907	15.8589	17.2400
	Chalak [18]	2.9721	3.6053	9.3976	10.7219	15.8489	17.2203
	3D Abaqus [41]	2.9674	3.6113	9.3738	10.7228	15.8337	17.5148
	ZIGT FE [41]	2.9791	3.6348	9.4418	10.8109	15.8500	17.3072
CSCS	Present	10.3848	15.3560	18.2338	21.4893	21.6985	26.7959
	Chalak [18]	10.3027	16.1798	18.3228	22.1962	23.2839	27.1750
	3D Abaqus [41]	10.2816	16.1245	18.3029	22.1480	23.1797	27.1464
	ZIGT FE [41]	10.3582	16.3499	18.3744	22.4100	23.5983	27.2300
CCCC	Present	11.3166	16.8330	19.1758	23.0592	23.7886	28.4357
	Chalak [18]	11.2607	16.7446	19.0385	22.8018	23.6414	28.1930
	3D Abaqus [41]	11.2236	16.6777	18.9650	22.7096	23.5270	28.0728
	ZIGT FE [41]	11.4158	17.0329	19.3780	23.4305	24.0862	28.7241

sandwich plates with lay-ups #1 and #2 with simply supported boundary conditions. The present method is compared against the analytical solutions based on the layer wise approach [20], the FEM solutions based on higher-order shear deformations theory [40], and other analytical solutions based on higher-order shear deformation theory with the ESL approach [13,14]. In these references, the effect of in-plane stresses are neglected so the results for the proposed method are presented for two cases: with and without in-plane stresses. The present formulation is in good agreement with the methods of the literature. Also, as expected, the natural frequencies decrease with the consideration of in-plane stresses.

The next comparison study is presented in Table 4, in which the first six dimensionless natural frequencies of a five-layer sandwich plate with lay-up #3 and four different boundary conditions (CCCC, CSCS, CFCF, and CFFF) are compared. The results of the present method are compared with the FEM results of Chalak et al. [18] based on higher-order zig-zag model, Kulkarni and Kapuria [41] based on zig-zag model for different boundary conditions, and 3 D results reported by Kulkarni and Kapuria [41]. Present results are in excellent agreement with those in the literature.

The last comparison study is devoted to the first six dimensionless natural frequencies of a five-layer simply supported sandwich plate with lay-up #4 as shown in Table 5. The results of the present method show a good agreement with the results by Rao et al. [15] and Wang et al. [42], who used the higher order mixed layer wise theory for both thin (a/h=10) and moderately thick (a/h=100) sandwich

Table 5. Dimensionless natural frequencies for anti-symmetric five-layer simply supported sandwich plates with lay-up #4, $a/b=1$, and $f_c/f_t=10$.

		Modes					
a/h	Method	1,1	1,2	2,2	1,3	2,3	3,3
10	Present	1.8444	3.2053	4.2585	5.1124	6.0607	7.0
	Rao et al. [15]	1.8480	3.2196	4.2867	5.2234	6.0942	7.6762
	Wang et al. [42]	1.8470	3.2182	4.2882	5.2286	6.0901	7.6721
	ESL [10]	4.8594	8.0187	10.2966	11.7381	13.4706	16.1320
100	Present	11.9515	23.4175	30.9631	36.1460	41.5612	49.5131
	Rao et al. [15]	11.9401	23.4017	30.9432	36.1434	41.4475	49.7622
	Wang et al. [42]	11.8593	23.3419	30.8647	36.1150	41.3906	49.7091
	ESL [10]	15.5093	39.0293	54.7618	72.7572	83.4412	105.3781

plates. Table 5 also gives the results obtained by ESL theory [10], which clearly overestimates the natural frequencies compared to the proposed model and the LW theory.

Effect of plate in-plane aspect ratio

To study the effect of the plate in-plane aspect ratio, we consider a seven-layer sandwich plate with soft flexible core, symmetric lay-up #1, and side-to-thickness $a/h = 10$. The core is made of HEREX-C70.130 PVC foam and the face sheets are made of glass polyester resin (corresponding to materials 1 and 2 of Table 1, respectively). Table 6 provides the first six dimensionless natural frequencies obtained for plates with aspect ratios $a/b=1$ and 2, subjected to different boundary conditions. It can be observed that the natural frequencies vary as expected with the changing of boundary conditions: for instance, the fully clamped plate has the highest frequencies, because in this case the general stiffness of the system is highest; conversely, when one side is clamped and the other three sides are free, the general stiffness is lowest, so the lowest frequencies are calculated. For the same boundary conditions, as the aspect ratio increases, the natural frequencies also increase.

In order to visualize the type of free vibrations of the sandwich plates with soft flexible core, the first six mode shapes of the symmetric sandwich plate with lay-up #1 for two boundary conditions (SSSS and SSSF) are shown in Figures 2 and 3.

Effect of boundary conditions

To investigate the effects of boundary conditions, we analyze an anti-symmetric sandwich plates with lay-up #2 and side-to-thickness ratio $a/h=10$. The adopted material properties are the same as in the previous example. The first four dimensionless natural frequencies of the plate subjected to different boundary conditions are shown in Figures 4 and 5 for aspect ratio $a/b = 1$ and 2, respectively. The

Table 6. Dimensionless natural frequencies for symmetric sandwich plates with lay-up #1, different boundary conditions, $a/h = 10$, and $h_c/h = 0.88$.

	B.C.	Dimensionless natural frequencies					
		ω_1	ω_2	ω_3	ω_4	ω_5	ω_6
$a/b = 1$	SSSS	14.2820	26.1842	26.8221	34.5165	39.1128	39.9223
	CCCC	17.9478	28.3883	28.8626	36.7106	40.9407	41.8097
	SSSF	10.4886	18.3217	24.8432	29.6955	31.1754	38.6135
	CFCF	12.8390	14.3070	23.8718	25.7326	27.7681	34.4752
	SCSC	16.1656	27.5669	27.6220	35.8010	40.4973	40.5721
	SSCF	10.9319	19.1317	24.9796	30.2877	32.0784	38.7532
	SFSF	12.7507	14.2018	23.7883	25.4969	27.5950	34.0244
	CCCF	13.6366	20.2508	26.3918	31.4783	32.6803	40.1626
	CFFF	4.0143	6.3308	15.2491	18.6960	19.9351	28.1375
	FFFF	10.1538	18.5966	20.3367	22.8370	23.8423	32.8215
$a/b = 2$	SSSS	26.1828	34.5131	45.1735	51.4412	55.5460	56.6561
	CCCC	29.9038	37.4583	47.8411	53.7021	58.0913	59.0258
	SSSF	12.4001	26.4037	36.1372	39.8191	43.1713	52.4893
	CFCF	12.8386	17.2968	25.7316	32.2413	39.6862	45.3543
	SCSC	29.1065	36.4640	46.8339	53.4658	57.6096	58.8917
	SSCF	15.2456	27.2396	36.9033	40.2578	44.0774	53.3827
	SFSF	12.7503	17.1937	25.4960	32.0918	39.3926	45.2257
	CCCF	17.0671	28.5307	37.2527	41.6105	44.8291	54.4597
	CFFF	4.0139	8.7116	15.2492	24.4851	30.5695	38.0243
	FFFF	16.5397	20.3260	30.6221	34.7169	43.5808	46.3031

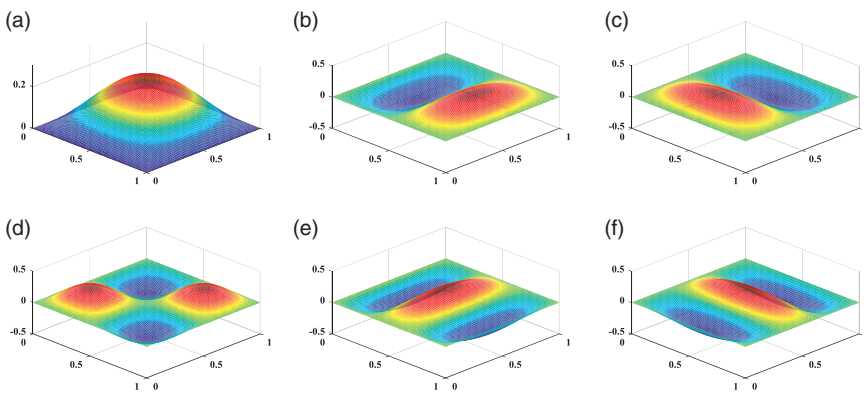

Figure 2. First six mode shapes of the seven-layer simply supported sandwich plate with lay-up #1, ($a/b = 1$) and ($a/h = 10$). (a) First mode (b) Second mode (c) Third mode (d) Fourth mode (e) Fifth mode (f) Sixth mode.

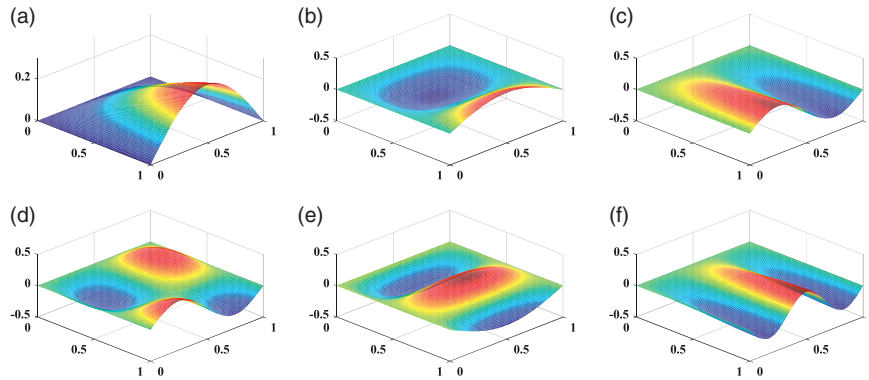

Figure 3. First six mode shapes of the seven-layer sandwich plate with SSSF boundary condition and lay-up #1, ($a/b = 1$) and (a/h=10). (a) First mode (b) Second mode (c) Third mode (d) Fourth mode (e) Fifth mode (f) Sixth mode.

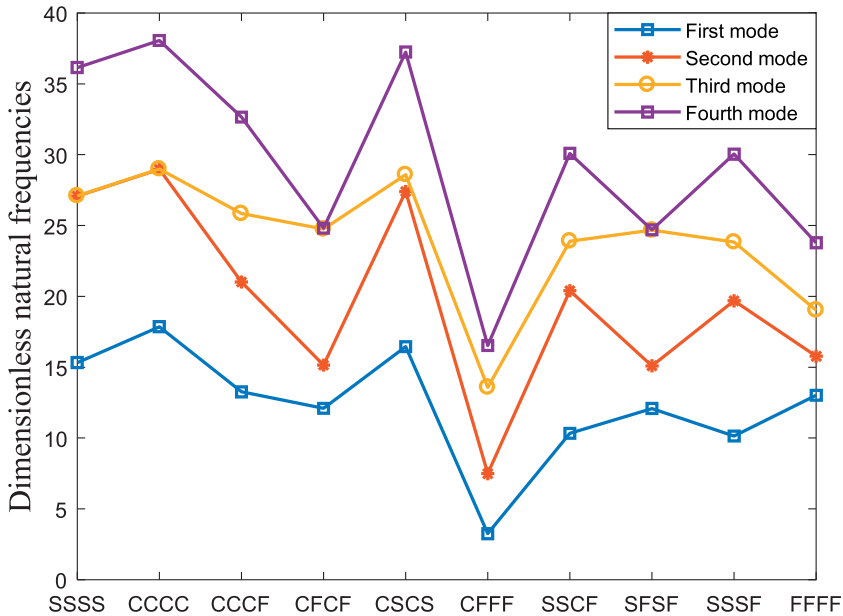

Figure 4. Dimensionless natural frequencies of the seven-layer anti-symmetric sandwich plate with lay-up #2 for different boundary conditions and a/b=1.

highest frequencies are obtained for the fully clamped (CCCC) boundary condition, while the lowest ones for the CFFF boundary condition. For the square plate (a/b=1), the natural frequencies of the second and third modes are the exactly same for the symmetric boundary conditions (CCCC and SSSS) and very close for the SCSC boundary condition. Besides, the third and fourth natural frequencies

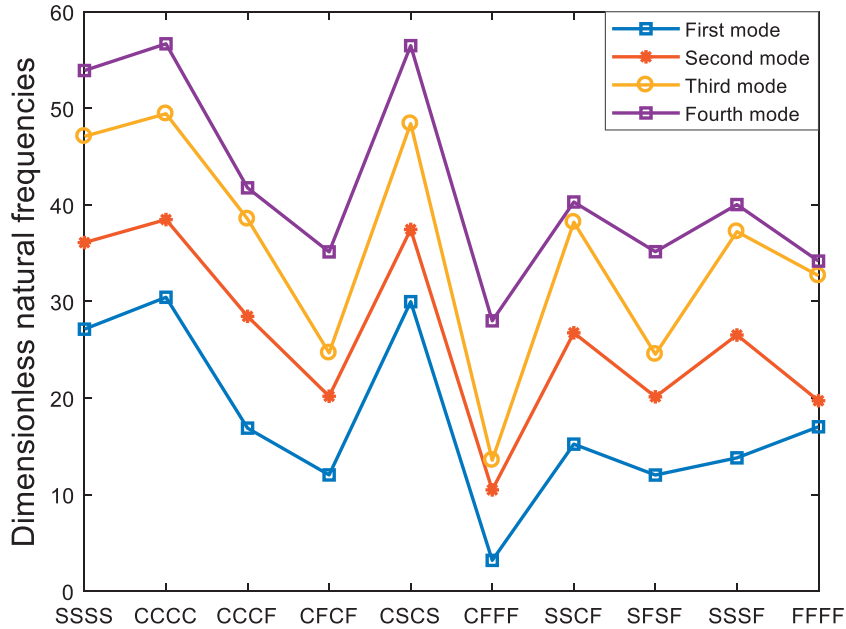

Figure 5. Dimensionless natural frequencies of the seven-layer anti-symmetric sandwich plate with lay-up #2 for different boundary conditions and a/b=2.

are very close for the CFCF and SFSF boundary conditions. Instead, for the rectangular plate ($a/b = 2$), the natural frequencies of two consecutive modes are always distinct for each of the boundary conditions.

The completely free boundary condition (FFFF) has received little attention in the literature. To further investigate this case, we analyze a square sandwich plate with completely free edges and lay-up ($0°/\theta/0°$/C/$0°/\theta/0°$), where θ can take the values 30°, 45°, 60°, and 90°. The material properties 1 and 2 of Table 1 are assumed for the core and face sheets, respectively. Table 7 shows the calculated dimensionless natural frequencies for different fiber-orientation angles and side-to-thickness aspect ratios.

Figure 6 shows the first six mode shapes for the plate with $a/h = 10$.

Effect of plate side-to-thickness ratio

Lastly, we investigate the effect of the plate side-to-thickness ratio. To this aim, we consider an anti-symmetric sandwich plate with lay-up #4 and soft flexible core. The material properties 5 and 6 of Table 1 are assumed for the core and face sheets, respectively. The first six natural frequencies calculated for different boundary conditions are presented in Table 8. Here, the side-to-thickness ratio is a/h= 20 and the core-to-face sheets thickness ratio is f_c/f_t= 10.

Table 7. Dimensionless natural frequencies of an all free (FFFF) square sandwich plate with symmetric lay-up 0°/θ/0°/C/0°/θ/0°.

a/h		Natural frequencies			
θ		30°	45°	60°	90°
10	ω_1	10.9743	11.1533	10.8147	10.1538
	ω_2	15.8724	16.4530	17.4125	18.5966
	ω_3	20.9667	20.6238	20.4126	20.3367
	ω_4	21.8127	22.1049	22.3183	22.8370
	ω_5	24.6524	24.6248	24.4309	23.8423
	ω_6	31.2163	31.7486	32.5704	32.8215
20	ω_1	13.1194	13.3655	12.8580	11.9376
	ω_2	18.7023	19.7119	21.3635	23.3447
	ω_3	28.4110	27.5812	27.0643	26.8776
	ω_4	29.2915	29.8605	30.0784	30.8875
	ω_5	35.3406	35.2716	34.7372	33.1645
	ω_6	45.2436	46.9761	49.5856	49.9988
30	ω_1	13.8523	14.1151	13.5538	12.5615
	ω_2	19.4245	20.5885	22.4728	24.6952
	ω_3	30.8871	29.8335	29.1757	28.9374
	ω_4	32.1515	32.8353	32.9965	33.8501
	ω_5	39.5914	39.5246	38.8033	36.6530
	ω_6	50.6153	53.1011	56.8301	57.8763
40	ω_1	14.2095	14.4779	13.8933	12.8733
	ω_2	19.7009	20.9353	22.9173	25.2281
	ω_3	31.9249	30.7672	30.0431	29.7801
	ω_4	33.5721	34.3100	34.4253	35.2717
	ω_5	41.6323	41.5811	40.7610	38.2813
	ω_6	53.1028	56.0003	60.3367	61.9881

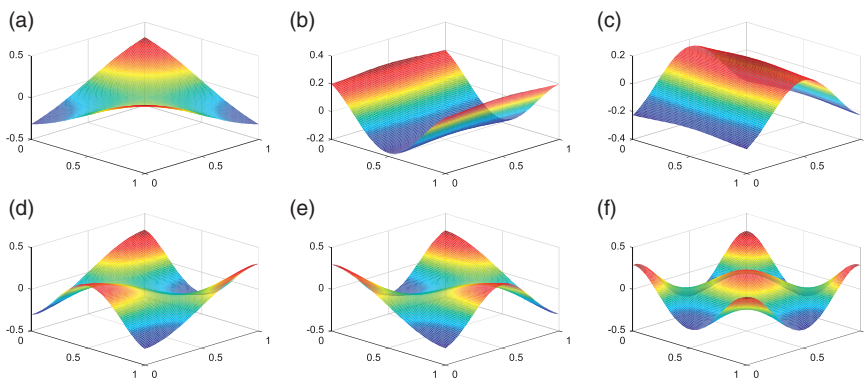

Figure 6. First six mode shapes of an all free (FFFF) square sandwich plate with lay-up #4 and $a/h = 10$. (a) First mode (b) Second mode (c) Third mode (d) Fourth mode (e) Fifth mode (f) Sixth mode.

Table 8. Dimensionless natural frequencies for a square anti-symmetric sandwich plate with lay-up #4, different boundary conditions, $a/b=1$, and $a/h=20$.

B.C.	Mode No.					
	ω_1	ω_2	ω_3	ω_4	ω_5	ω_6
SSSS	3.4789	5.7273	5.7333	7.3888	8.5296	8.5701
CCCC	3.9141	6.3522	6.3605	8.1863	9.4472	9.5067
SSSF	2.6613	4.4447	5.2764	6.4272	6.9962	8.2089
CFCF	2.7489	3.4485	5.6713	5.8415	6.1924	7.7812
SCSC	3.7006	5.8729	6.2264	7.9586	9.3051	9.3687
SSCF	2.7506	4.6222	5.3044	6.6277	7.3212	8.3133
SFSF	2.7479	3.4485	5.6678	5.8303	6.1960	8.4340
CCCF	3.0290	4.7929	5.8285	7.0012	7.4522	9.0654
CFFF	1.2345	1.9263	3.8246	4.5494	5.2021	6.5562
FFFF	3.1368	5.0134	5.0177	5.6310	5.6955	7.4512

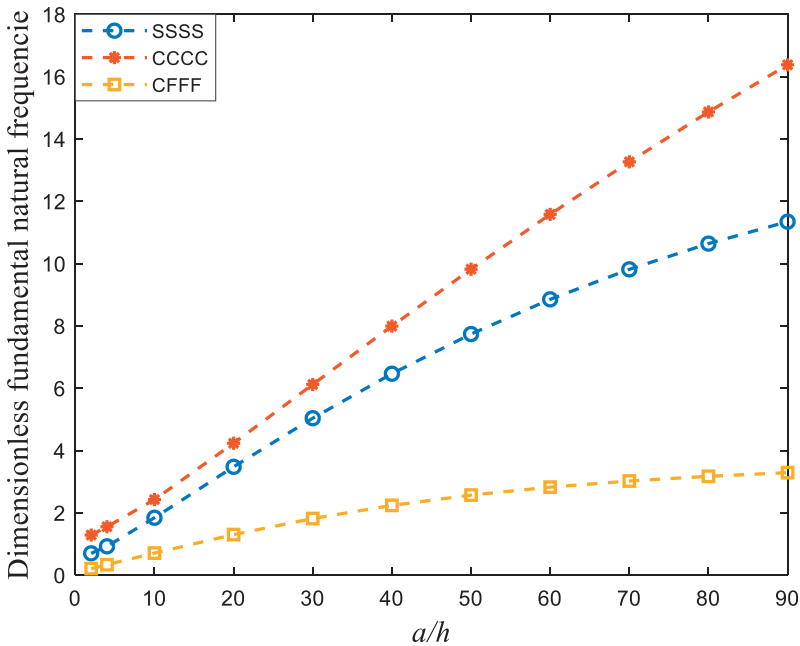

Figure 7. Fundamental natural frequency of a square sandwich plate with lay-up #4 as a function of the side-to-thickness ratio.

Figure 7 displays the variation of the first natural frequency with the plate side-to-thickness ratio. Three different boundary conditions (SSSS, CCCC, and CFFF) are analyzed. As the side-to-thickness ratio increases, the first natural frequency increases. Indeed, the moderately thick sandwich plates have lower frequencies with respect to the thinner plates.

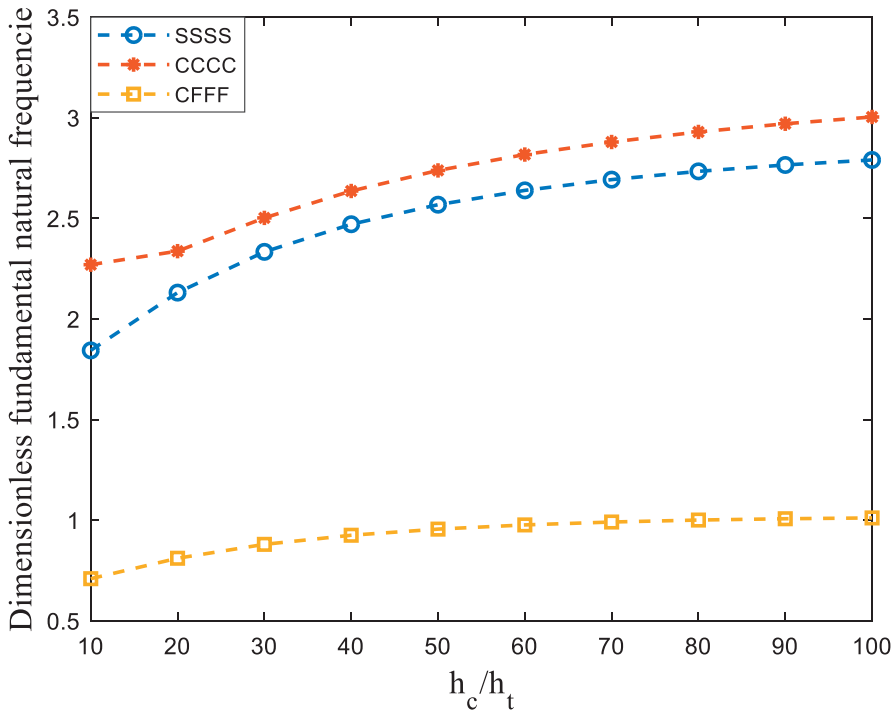

Figure 8. Fundamental natural frequency of a square sandwich plate with lay-up (0/90/C/0/90) as a function of the core-to face sheets thickness ratio.

Effect of core-to-face sheets thickness ratio

Figure 8 illustrates the effect of the core-to-face sheets thickness ratio on the first natural frequency of a square sandwich plate for the SSSS, CCCC and CFFF boundary conditions. As shown in the figure, with the increase of this ratio, the first natural frequency increases for all of the three boundary conditions considered. Again, the fully clamped sandwich plate has the highest fundamental natural frequency among the other boundary conditions.

Conclusions

We analyzed the free vibrations of composite sandwich plates with compressible core via an extended higher-order sandwich panel theory (EHSAPT). The governing equations were derived by using Hamilton's principle. The Rayleigh-Ritz method with two-variable orthogonal polynomials was used for the solution in terms of natural frequencies and mode shapes. The free vibrations of sandwich plates with both symmetric and anti-symmetric lay-ups subjected to various boundary conditions were investigated. Results were validated with previous results from the literature and excellent agreement was observed. Eventually, the

effects were investigated of various parameters such as the plate in-plane ratio, boundary conditions, plate side-to-thickness ratio, and core-to-face sheets thickness ratio. The results show that the fundamental natural frequencies increase with both the plate in-plane ratio and side-to-thickness ratio, as well as with the core-to-face sheets thickness ratio. For an all free square plate, the effect was also examined of changing the fiber orientation angle in the face sheets.

Declaration of Conflicting Interests

The author(s) declared no potential conflicts of interest with respect to the research, authorship, and/or publication of this article.

Funding

The author(s) disclosed receipt of the following financial support for the research, authorship and/or publication of this article: The first three authors acknowledge the funding support of Babol Noshirvani University of Technology through Grant program No. BNUT/964113035/96.

ORCID iDs

Ramazan-Ali Jafari-Talookolaei https://orcid.org/0000-0003-4357-2597
Paolo S Valvo https://orcid.org/0000-0001-6439-1926

References

1. Vinson JR. *Plate and panel structures of isotropic, composite and piezoelectric materials, including sandwich construction*. Berlin: Springer Science & Business Media, 2006.
2. Altenbach H, Altenbach J and Kissing W. *Mechanics of composite structural elements*. Berlin: Springer, 2018.
3. Srinivas S, Rao AK and Rao CJ. Flexure of simply supported thick homogeneous and laminated rectangular plates. *ZAMM – J Appl Math Mech/Z Angew Math Mech* 1969; 49: 449–458.
4. Srinivas S, Rao CJ and Rao A. An exact analysis for vibration of simply-supported homogeneous and laminated thick rectangular plates. *J Sound Vib* 1970; 12: 187–199.
5. Srinivas S and Rao A. Bending, vibration and buckling of simply supported thick orthotropic rectangular plates and laminates. *Int J Solids Struct* 1970; 6: 1463–1481.
6. Pagano NJ. Exact solutions for rectangular bidirectional composites and sandwich plates. *J Compos Mater* 1970; 4: 20–34.
7. Noor AK, Peters JM and Burton WS. Three-dimensional solutions for initially stressed structural sandwiches. *J Eng Mech* 1994; 120: 284–303.
8. Reddy JN. A simple higher-order theory for laminated composite plates. *J Appl Mech* 1984; 51: 745–752.
9. Kant T and Swaminathan K. Analytical solutions for the static analysis of laminated composite and sandwich plates based on a higher order refined theory. *Compos Struct* 2002; 56: 329–344.
10. Kant T and Swaminathan K. Analytical solutions for free vibration of laminated composite and sandwich plates based on a higher-order refined theory. *Compos Struct* 2001; 53: 73–85.

11. Swaminathan K, Patil S, Nataraja M, et al. Bending of sandwich plates with antisymmetric angle-ply face sheets–analytical evaluation of higher order refined computational models. *Compos Struct* 2006; 75: 114–120.
12. Swaminathan K and Patil S. Analytical solutions using a higher order refined computational model with 12 degrees of freedom for the free vibration analysis of antisymmetric angle-ply plates. *Compos Struct* 2008; 82: 209–216.
13. Meunier M and Shenoi R. Dynamic analysis of composite sandwich plates with damping modelled using high-order shear deformation theory. *Compos Struct* 2001; 54: 243–254.
14. Nayak A, Moy S and Shenoi R. Free vibration analysis of composite sandwich plates based on Reddy's higher-order theory. *Compos Part B Eng* 2002; 33: 505–519.
15. Rao M and Desai Y. Analytical solutions for vibrations of laminated and sandwich plates using mixed theory. *Compos Struct* 2004; 63: 361–373.
16. Bardell N, Dunsdon J and Langley R. Free vibration analysis of coplanar sandwich panels. *Compos Struct* 1997; 38: 463–475.
17. Yang C, Jin G, Ye X, et al. A modified Fourier–Ritz solution for vibration and damping analysis of sandwich plates with viscoelastic and functionally graded materials. *Int J Mech Sci* 2016; 106: 1–18.
18. Chalak H, Chakrabarti A, Iqbal MA, et al. Free vibration analysis of laminated soft core sandwich plates. *J Vib Acoust* 2013; 135: 011013.
19. Frostig Y and Thomsen OT. High-order free vibration of sandwich panels with a flexible core. *Int J Solids Struct* 2004; 41: 1697–1724.
20. Malekzadeh K, Khalili M and Mittal R. Local and global damped vibrations of plates with a viscoelastic soft flexible core: an improved high-order approach. *J Sandwich Struct Mater* 2005; 7: 431–456.
21. Malekzadeh K and Sayyidmousavi A. Free vibration analysis of sandwich plates with a uniformly distributed attached mass, flexible core, and different boundary conditions. *J Sandwich Struct Mater* 2010; 12: 709–732.
22. Frostig Y, Phan C and Kardomateas G. Free vibration of unidirectional sandwich panels, part I: compressible core. *J Sandwich Struct Mater* 2013; 15: 377–411.
23. Ritz W. Uber eine neue methode zur losung gewisser variationsprobleme der mathematischen physik. *J Math* 1909; 135: 1–61.
24. Ritz W. Theorie der transversalschwingungen einer quadratischen platte mit freien rändern. *Ann Phys* 1909; 333: 737–786.
25. Rahmani O, Khalili S and Malekzadeh K. Free vibration response of composite sandwich cylindrical shell with flexible core. *Compos Struct* 2010; 92: 1269–1281.
26. Abedi M, Jafari-Talookolaei R-A and Valvo PS. A new solution method for free vibration analysis of rectangular laminated composite plates with general stacking sequences and edge restraints. *Comput Struct* 2016; 175: 144–156.
27. Bhat R. Natural frequencies of rectangular plates using characteristic orthogonal polynomials in Rayleigh-Ritz method. *J Sound Vib* 1985; 102: 493–499.
28. Bhat R. Flexural vibration of polygonal plates using characteristic orthogonal polynomials in two variables. *J Sound Vib* 1987; 114: 65–71.
29. Liew K, Lam K and Chow S. Free vibration analysis of rectangular plates using orthogonal plate function. *Comput Struct* 1990; 34: 79–85.
30. Liew K, Xiang Y, Kitipornchai S, et al. Vibration of thick skew plates based on Mindlin shear deformation plate theory. *J Sound Vib* 1993; 168: 39–69.

31. Nallim LG, Martinez SO and Grossi RO. Statical and dynamical behaviour of thin fibre reinforced composite laminates with different shapes. *Comput Methods Appl Mech Eng* 2005; 194: 1797–1822.
32. Nallim LG and Oller S. An analytical–numerical approach to simulate the dynamic behaviour of arbitrarily laminated composite plates. *Compos Struct* 2008; 85: 311–325.
33. Rango RF, Bellomo FJ and Nallim LG. A variational Ritz formulation for vibration analysis of thick quadrilateral laminated plates. *Int J Mech Sci* 2015; 104: 60–74.
34. Kumar Y and Lal R. Vibrations of nonhomogeneous orthotropic rectangular plates with bilinear thickness variation resting on Winkler foundation. *Meccanica* 2012; 47: 893–915.
35. Behera L and Chakraverty S. Effect of scaling effect parameters on the vibration characteristics of nanoplates. *J Vib Control* 2016; 22: 2389–2399.
36. Kumar Y. The Rayleigh–Ritz method for linear dynamic, static and buckling behavior of beams, shells and plates: a literature review. *J Vib Control* 2018; 24: 1205–1227.
37. Moreno-García P, dos Santos JVA and Lopes H. A review and study on Ritz method admissible functions with emphasis on buckling and free vibration of isotropic and anisotropic beams and plates. *Arch Comput Methods Eng* 2018; 25: 785–815.
38. Nallim L and Grossi R. On the use of orthogonal polynomials in the study of anisotropic plates. *J Sound Vib* 2003; 264: 1201–1207.
39. Jones R. *Mechanics of composite materials*. 2nd ed. Philadelphia, PA: Taylor & Francis, 1999.
40. Belarbi M-O, Tati A, Ounis H, et al. On the free vibration analysis of laminated composite and sandwich plates: a layerwise finite element formulation. *Lat Am J Solids Struct* 2017; 14: 2265–2290.
41. Kulkarni S and Kapuria S. Free vibration analysis of composite and sandwich plates using an improved discrete Kirchhoff quadrilateral element based on third-order zigzag theory. *Comput Mech* 2008; 42: 803–824.
42. Wang T, Sokolinsky V, Rajaram S, et al. Consistent higher-order free vibration analysis of composite sandwich plates. *Compos Struct* 2008; 82: 609–621.

Appendix 1

The first members of the basic functions classes can be defined as follows:

(a) For the transverse displacements:

$$\phi_1^{w\alpha} = x^{\beta_1} y^{\beta_2} (x-a)^{\beta_3} (y-b)^{\beta_4} \tag{31}$$

where $\alpha = t, b, c$ and

$$\beta_i = \begin{cases} 0 & \text{if edge } i \text{ is free} \\ 1 & \text{if edge } i \text{ is simply supported} \\ 2 & \text{if edge } i \text{ is clamped} \end{cases}$$

(b) For the x-displacements and rotations:

$$\phi_1^{u^\alpha} = x^{\gamma_1} y^{\gamma_2} (x-a)^{\gamma_3} (y-b)^{\gamma_4} \tag{32}$$

and:

$$\phi_1^{x^t} = \phi_1^{x^b} = \phi_1^{u_1{}^c} = \phi_1^{u^\alpha} \tag{33}$$

where $\alpha = t, b, c$ and:

$$\gamma_i = \begin{cases} 0 & \text{if edge } i \text{ is free or simply supported in y} - \text{direction} \\ 1 & \text{if edge } i \text{ is simply supported in x} - \text{direction or clamped} \end{cases}$$

(c) For the y-displacements and rotations:

$$\phi_1^{v^\alpha} = x^{\delta_1} y^{\delta_2} (x-a)^{\delta_3} (y-b)^{\delta_4} \tag{34}$$

and:

$$\phi_1^{y^t} = \phi_1^{y^b} = \phi_1^{v_1{}^c} = \phi_1^{v^\alpha} \tag{35}$$

where $\alpha = t, b, c$ and:

$$\delta_i = \begin{cases} 0 & \text{if edge } i \text{ is free or simply supported in x} - \text{direction} \\ 1 & \text{if edge } i \text{ is simply supported in y} - \text{direction or clamped} \end{cases}$$

Appendix 2

The governing differential equations along with the boundary conditions can be derived by using Hamilton's principle:

$$\int_{t_1}^{t_2} (\delta T - \delta U) dt = 0 \tag{36}$$

where t_1 and t_2 are the values of time at the beginning and end of motion, respectively. By substituting equations (19) and (20) into (B-1), the governing equations are derived:

$$
\begin{aligned}
&N^t_{xx,x}+N^t_{xy,y}+\frac{2}{f_c^2}M^c_{2xx,x}+\frac{2}{f_c^2}M^c_{2xy,y}-\frac{4}{f_c^2}M^c_{Q1xz}-\frac{4}{f_c^3}M^c_{3xx,x}-\frac{4}{f_c^3}M^c_{3xy,y}\\
&\quad+\frac{12}{f_c^3}M^c_{Q2xz}-I^t_0u^t_{0,tt}-I^t_1\psi^t_{x,tt}-\frac{4}{f_c^3}I^c_3u_{0,tt}+\frac{2}{f_c^2}I^c_2u_{0,tt}-\frac{4}{f_c^3}I^c_4u_{1,tt}+\frac{2}{f_c^2}I^c_3u_{1,tt}\\
&\quad-\frac{4}{f_c^3}I^c_5u_{2,tt}+\frac{2}{f_c^2}I^c_4u_{2,tt}-\frac{4}{f_c^3}I^c_6u_{3,tt}+\frac{2}{f_c^2}I^c_5u_{3,tt}=0\\
&N^b_{xx,x}+N^b_{xy,y}+\frac{2}{f_c^2}M^c_{2xx,x}+\frac{2}{f_c^2}M^c_{2xy,y}-\frac{4}{f_c^2}M^c_{Q1xz}-\frac{4}{f_c^3}M^c_{3xx,x}+\frac{4}{f_c^3}M^c_{3xy,y}\\
&\quad-\frac{12}{f_c^3}M^c_{Q2xz}-I^b_0u^b_{0,tt}-I^b_1\psi^b_{x,tt}+\frac{4}{f_c^3}I^c_3u_{0,tt}+\frac{2}{f_c^2}I^c_2u_{0,tt}+\frac{4}{f_c^3}I^c_4u_{1,tt}+\frac{2}{f_c^2}I^c_3u_{1,tt}\\
&\quad+\frac{4}{f_c^3}I^c_5u_{2,tt}+\frac{2}{f_c^2}I^c_4u_{2,tt}+\frac{4}{f_c^3}I^c_6u_{3,tt}+\frac{2}{f_c^2}I^c_5u_{3,tt}=0\\
&M^t_{xx,x}+M^t_{xy,y}-Q^t_{xz}+\frac{f_t}{f_c^2}M^c_{2xx,x}+\frac{f_t}{f_c^2}M^c_{2xy,y}-2\frac{f_t}{f_c^2}M^c_{Q1xz}-2\frac{f_t}{f_c^3}M^c_{3xx,x}\\
&\quad-2\frac{f_t}{f_c^3}M^c_{3xy,y}+6\frac{f_t}{f_c^3}M^c_{Q2xz}-I^t_1u^t_{0,tt}-I^t_2\psi^t_{x,tt}-2\frac{f_t}{f_c^3}I^c_3u_{0,tt}+\frac{f_t}{f_c^2}I^c_2u_{0,tt}-2\frac{f_t}{f_c^3}I^c_4u_{1,tt}\\
&\quad+\frac{f_t}{f_c^2}I^c_3u_{1,tt}-2\frac{f_t}{f_c^3}I^c_5u_{2,tt}+\frac{f_t}{f_c^2}I^c_4u_{2,tt}-2\frac{f_t}{f_c^3}I^c_6u_{3,tt}+\frac{f_t}{f_c^2}I^c_5u_{3,tt}=0\\
&M^b_{xx,x}+M^b_{xy,y}-Q^b_{xz}-\frac{f_b}{f_c^2}M^c_{2xx,x}-\frac{f_b}{f_c^2}M^c_{2xy,y}+2\frac{f_b}{f_c^2}M^c_{Q1xz}-2\frac{f_b}{f_c^3}M^c_{3xx,x}\\
&\quad-2\frac{f_b}{f_c^3}M^c_{3xy,y}+6\frac{f_b}{f_c^3}M^c_{Q2xz}-I^b_1u^b_{0,tt}-I^b_2\psi^b_{x,tt}-2\frac{f_b}{f_c^3}I^c_3u_{0,tt}-\frac{f_b}{f_c^2}I^c_2u_{0,tt}\\
&\quad-2\frac{f_b}{f_c^3}I^c_4u_{1,tt}-\frac{f_b}{f_c^2}I^c_3u_{1,tt}-2\frac{f_b}{f_c^3}I^c_5u_{2,tt}-\frac{f_b}{f_c^2}I^c_4u_{2,tt}-2\frac{f_b}{f_c^3}I^c_6u_{3,tt}-\frac{f_b}{f_c^2}I^c_5u_{3,tt}=0\\
&Q^t_{xz,x}+Q^t_{yz,y}-\frac{1}{f_c}M^c_{Q1yz,y}-\frac{1}{f_c}M^c_{Q1xz,x}+\frac{1}{f_c}R^c_Z+\frac{2}{f_c^2}M^c_{Q2yz,y}+\frac{2}{f_c^2}M^c_{Q2xz,x}\\
&\quad-\frac{4}{f_c^2}M^c_z-I^t_0w^t_{0,tt}-\frac{1}{f_c}I^c_1w_{0,tt}+\frac{2}{f_c^2}I^c_2w_{0,tt}-\frac{1}{f_c}I^c_2w_{1,tt}+\frac{2}{f_c^2}I^c_3w_{1,tt}\\
&\quad-\frac{1}{f_c}I^c_3w_{2,tt}+\frac{2}{f_c^2}I^c_4w_{2,tt}=0\\
&Q^b_{xz,x}+Q^b_{yz,y}+\frac{1}{f_c}M^c_{Q1yz,y}+\frac{1}{f_c}M^c_{Q1xz,x}-\frac{1}{f_c}R^c_Z+\frac{2}{f_c^2}M^c_{Q2yz,y}+\frac{2}{f_c^2}M^c_{Q2xz,x}\\
&\quad-\frac{4}{f_c^2}M^c_z-I^b_0w^b_{0,tt}+\frac{1}{f_c}I^c_1w_{0,tt}+\frac{2}{f_c^2}I^c_2w_{0,tt}+\frac{1}{f_c}I^c_2w_{1,tt}+\frac{2}{f_c^2}I^c_3w_{1,tt}+\frac{1}{f_c}I^c_3w_{2,tt}+\frac{2}{f_c^2}I^c_4w_{2,tt}=0
\end{aligned}
$$

$$N^t_{yy,y}+N^t_{xy,x}+\frac{2}{f^2_c}M^c_{2yy,y}+\frac{2}{f^2_c}M^c_{2xy,x}-\frac{4}{f^2_c}M^c_{Q1yz}-\frac{4}{f^3_c}M^c_{3yy,y}-\frac{4}{f^3_c}M^c_{3xy,x}+\frac{12}{f^3_c}M^c_{Q2yz}$$
$$-I^t_0v^t_{0,tt}-I^t_1\psi^t_{y,tt}-\frac{4}{f^3_c}I^c_3v_{0,tt}+\frac{2}{f^2_c}I^c_2v_{0,tt}-\frac{4}{f^3_c}I^c_4v_{1,tt}+\frac{2}{f^2_c}I^c_3v_{1,tt}-\frac{4}{f^3_c}I^c_5v_{2,tt}+\frac{2}{f^2_c}I^c_4v_{2,tt}$$
$$-\frac{4}{f^3_c}I^c_6v_{3,tt}+\frac{2}{f^2_c}I^c_5v_{3,tt}=0$$
$$N^b_{yy,y}+N^b_{xy,x}+\frac{2}{f^2_c}M^c_{2yy,y}+\frac{2}{f^2_c}M^c_{2xy,x}-\frac{4}{f^2_c}M^c_{Q1yz}+\frac{4}{f^3_c}M^c_{3yy,y}+\frac{4}{f^3_c}M^c_{3xy,x}$$
$$-\frac{12}{f^3_c}M^c_{Q2yz}-I^b_0v^b_{0,tt}-I^b_1\psi^b_{y,tt}+\frac{4}{f^3_c}I^c_3v_{0,tt}+\frac{2}{f^2_c}I^c_2v_{0,tt}+\frac{4}{f^3_c}I^c_4v_{1,tt}+\frac{2}{f^2_c}I^c_3v_{1,tt}$$
$$+\frac{4}{f^3_c}I^c_5v_{2,tt}+\frac{2}{f^2_c}I^c_4v_{2,tt}+\frac{4}{f^3_c}I^c_6v_{3,tt}+\frac{2}{f^2_c}I^c_5v_{3,tt}=0$$
$$M^t_{yy,y}+M^t_{xy,x}-Q^t_{yz}+\frac{f_t}{f^2_c}M^c_{2yy,y}+\frac{f_t}{f^2_c}M^c_{2xy,x}-2\frac{f_t}{f^2_c}M^c_{Q1yz}-2\frac{f_t}{f^3_c}M^c_{3yy,y}-2\frac{f_t}{f^3_c}M^c_{3xy,x}$$
$$+6\frac{f_t}{f^3_c}M^c_{Q2yz}-I^t_1v^t_{0,tt}-I^t_2\psi^t_{y,tt}-2\frac{f_t}{f^3_c}I^c_3v_{0,tt}+\frac{f_t}{f^2_c}I^c_2v_{0,tt}-2\frac{f_t}{f^3_c}I^c_4v_{1,tt}+\frac{f_t}{f^2_c}I^c_3v_{1,tt}$$
$$-2\frac{f_t}{f^3_c}I^c_5v_{2,tt}+\frac{f_t}{f^2_c}I^c_4v_{2,\mathrm{t}t}-2\frac{f_t}{f^3_c}I^c_6v_{3,tt}+\frac{f_t}{f^2_c}I^c_5v_{3,tt}=0$$
$$M^b_{yy,y}+M^b_{xy,x}-Q^b_{yz}-\frac{f_b}{f^2_c}M^c_{2yy,y}-\frac{f_b}{f^2_c}M^c_{2xy,x}+2\frac{f_b}{f^2_c}M^c_{Q1yz}-2\frac{f_b}{f^3_c}M^c_{3yy,y}-2\frac{f_b}{f^3_c}M^c_{3xy,x}$$
$$+6\frac{f_v}{f^3_c}M^c_{Q2yz}-I^t_1v^t_{0,tt}-I^t_2\psi^t_{y.tt}-2\frac{\mathrm{f}_b}{f^3_c}I^c_3v_{0,tt}-\frac{f_b}{f^2_c}I^c_2v_{0,tt}-2\frac{f_b}{f^3_c}I^c_4v_{1,tt}-\frac{f_b}{f^2_c}I^c_3v_{1,tt}$$
$$-2\frac{f_b}{f^3_c}I^c_5v_{2,tt}-\frac{f_b}{f^2_c}I^c_4v_{2,tt}-2\frac{f_b}{f^3_c}I^c_6v_{3,tt}-\frac{f_b}{f^2_c}I^c_5v_{3,tt}=0$$
$$Q^c_{yz,y}+Q^c_{xz,x}-\frac{4}{f^2_c}M^c_{Q2yz,y}-\frac{4}{f^2_c}M^c_{Q2xz,x}+\frac{8}{f^2_c}M^c_z-I^c_0w_{0,tt}-\frac{4}{f^2_c}I^c_2w_{0,tt}-I^c_1w_{1,tt}$$
$$-\frac{4}{f^2_c}I^c_3w_{1,tt}-I^c_2w_{2,tt}-\frac{4}{f^2_c}I^c_4w_{2,tt}=0$$
$$M^c_{yy.y}+M^c_{xy.x}-Q^c_{yz}-\frac{4}{f^2_c}M^c_{3yy,y}-\frac{4}{f^2_c}M^c_{3xy,x}+\frac{12}{f^2_c}M^c_{Q2yz}-I^c_1v_{0,tt}$$
$$-\frac{4}{f^2_c}I^c_3v_{0,tt}-I^c_2v_{1,tt}-\frac{4}{f^2_c}I^c_4v_{1,tt}-I^c_3v_{2,tt}-\frac{4}{f^2_c}I^c_5v_{2,tt}-I^c_4v_{3,tt}-\frac{4}{f^2_c}I^c_6v_{3,tt}=0$$
$$M^c_{xx,x}+M^c_{xy,y}-Q^c_{xz}-\frac{4}{f^2_c}M^c_{3xx,x}-\frac{4}{f^2_c}M^c_{3xy,y}+\frac{12}{f^2_c}M^c_{Q2xz}-I^c_1u_{0,tt}-\frac{4}{f^2_c}I^c_3u_{0,tt}$$
$$-I^c_2u_{1,tt}-\frac{4}{f^2_c}I^c_4u_{1,tt}-I^c_3u_{2,tt}-\frac{4}{f^2_c}I^c_5u_{2,tt}-I^c_4u_{3,tt}-\frac{4}{f^2_c}I^c_6u_{3,tt}=0$$
$$N^c_{xx,x}+N^c_{xy,y}-\frac{4}{f^2_c}M^c_{2xx,x}-\frac{4}{f^2_c}M^c_{2xy,y}+\frac{8}{f^2_c}M^c_{Q1xz}-I^c_0u_{0,tt}-\frac{4}{f^2_c}I^c_2u_{0,tt}$$
$$-I^c_1u_{1,tt}-\frac{4}{f^2_c}I^c_3u_{1,tt}-I^c_2u_{2,tt}-\frac{4}{f^2_c}I^c_4u_{2,tt}-I^c_3u_{3,\mathrm{t}t}-\frac{4}{f^2_c}I^c_5u_{3,tt}=0$$
$$N^c_{yy,y}+N^c_{xy,x}-\frac{4}{f^2_c}M^c_{2yy,y}-\frac{4}{f^2_c}M^c_{2xy,x}+\frac{8}{f^2_c}M^c_{Q1yz}-I^c_0v_{0,tt}$$

$$-\frac{4}{f_c^2}I_2^c v_{0,tt} - I_1^c v_{1,tt} - \frac{4}{f_c^2}I_3^c v_{1,tt} - I_2^c v_{2,tt} - \frac{4}{f_c^2}I_4^c v_{2,tt} - I_3^c v_{3,tt} - \frac{4}{f_c^2}I_5^c v_{3,tt} = 0 \tag{B-2}$$

Along with the boundary conditions:

$$\begin{aligned}
&At\ x = 0\ and\ x = a: \\
&N_{xx}^i = 0\ or\ u_0^i = 0; \quad M_{xx}^i = 0\ or\ \psi_x^i = 0; \quad N_{xy}^i = 0\ or\ v_0^i = 0\ ; \\
&M_{xy}^i = 0\ or\ \psi_y^i = 0; \quad Q_{xz}^i = 0\ or\ w_0^i = 0; \quad M_{Q1xz}^i = 0\ or\ w_1 = 0; \\
&M_{xz}^i = 0\ or\ w_2 = 0; \quad Q_{xz}^c = 0\ or\ w_0 = 0; \quad N_{xx}^c = 0\ or\ u_0 = 0; \\
&M_{xx}^c = 0\ or\ u_1 = 0; \quad M_{2xx}^c = 0\ or\ u_2 = 0; \quad M_{3xx}^c = 0\ or\ u_3 = 0\ ; \\
&N_{xy}^c = 0\ or\ v_0 = 0; \quad M_{xy}^c = 0\ or\ v_1 = 0; \quad M_{2xy}^c = 0\ or\ v_2 = 0\ ; \\
&M_{3xy}^c = 0\ or\ v_3 = 0; \quad \text{AT}\ y = 0\ and\ y = a: N_{yy}^i = 0\ or\ v_0^i = 0; \\
&M_{yy}^i = 0\ or\ \psi_y^i = 0; \quad N_{xy}^i = 0\ or\ u_0^i = 0; \ M_{xy}^i = 0\ or\ \psi_y^i = 0; \\
&Q_{yz}^i = 0\ or\ w_0^i = 0; \quad M_{Q1yz}^c = 0\ or\ w_1 = 0; \ M_{Q2yz}^c = 0\ or\ w_2 = 0; \\
&Q_{yz}^c = 0\ or\ w_0 = 0; \quad N_{xy}^c = 0\ or\ u_0 = 0; \ M_{xy}^c = 0\ or\ u_1 = 0; \\
&M_{2xy}^c = 0\ or\ u_2 = 0; \quad M_{3xy}^c = 0\ or\ u_3 = 0; \ N_{yy}^c = 0\ or\ v_0 = 0; \\
&M_{yy}^c = 0\ or\ v_1 = 0; \quad M_{2yy}^c = 0\ or\ v_2 = 0; \ M_{3yy}^c = 0\ or\ v_3 = 0\ ;
\end{aligned} \tag{38}$$